SN 2023emq: a probable flash-ionised Ibn supernova

M. Pursiainen ,[1] G. Leloudas ,[1] S. Schulze ,[2] P. Charalampopoulos ,[3] C. R. Angus ,[4]
J. P. Anderson ,[5, 6] F. Bauer ,[7, 8, 6] T.-W. Chen ,[9] L. Galbany ,[10, 11] M. Gromadzki ,[12]
C. P. Gutiérrez ,[13, 14] C. Inserra ,[15] T. E. Müller-Bravo ,[10] M. Nicholl ,[16] S. J. Smartt ,[17, 16]
L. Tartaglia ,[18] P. Wiseman ,[19] and D. R. Young [16]

[1] DTU Space, National Space Institute, Technical University of Denmark, Elektrovej 327, 2800 Kgs. Lyngby, Denmark
[2] The Oskar Klein Centre, Department of Physics, Stockholm University, AlbaNova, SE-10691 Stockholm, Sweden
[3] Department of Physics and Astronomy, University of Turku, FI-20014 Turku, Finland
[4] DARK, Niels Bohr Institute, University of Copenhagen, Copenhagen, Denmark
[5] European Southern Observatory, Alonso de Córdova 3107, Casilla 19, Santiago, Chile
[6] Millennium Institute of Astrophysics MAS, Nuncio Monsenor Sotero Sanz 100, Off. 104, Providencia, Santiago, Chile
[7] Instituto de Astrofísica, Facultad de Física, Pontificia Universidad Católica de Chile, Campus San Joaquín, Av. Vicuña Mackenna 4860, Macul Santiago, Chile, 7820436
[8] Centro de Astroingeniería, Facultad de Física, Pontificia Universidad Católica de Chile, Campus San Joaquín, Av. Vicuña Mackenna 4860, Macul Santiago, Chile, 7820436
[9] Technische Universität München, TUM School of Natural Sciences, Physik-Department, James-Franck-Straße 1, 85748 Garching, Germany
[10] Institute of Space Sciences (ICE, CSIC), Campus UAB, Carrer de Can Magrans, s/n, E-08193 Barcelona, Spain
[11] Institut d'Estudis Espacials de Catalunya (IEEC), E-08034 Barcelona, Spain
[12] Astronomical Observatory, University of Warsaw, Al. Ujazdowskie 4, 00-478 Warszawa, Poland
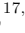[13] Institut d'Estudis Espacials de Catalunya, Gran Capità, 2-4, Edifici Nexus, Desp. 201, E-08034 Barcelona, Spain
[14] Institute of Space Sciences (ICE, CSIC), Campus UAB, Carrer de Can Magrans, s/n, E-08193 Barcelona, Spain
[15] Cardiff Hub for Astrophysics Research and Technology, School of Physics & Astronomy, Cardiff University, Queens Buildings, The Parade, Cardiff, CF24 3AA, UK
[16] Astrophysics Research Centre, School of Mathematics and Physics, Queens University Belfast, Belfast BT7 1NN, UK
[17] Department of Physics, University of Oxford, Keble Road, Oxford, OX1 3RH, UK
[18] INAF - Osservatorio Astronomico d'Abruzzo, via M. Maggini snc, I-64100 Teramo, Italy
[19] School of Physics and Astronomy, University of Southampton, Southampton, SO17 1BJ, UK

ABSTRACT

SN 2023emq is a fast-evolving transient initially classified as a rare Type Icn supernova (SN), interacting with a H- and He-free circumstellar medium (CSM) around maximum light. Subsequent spectroscopy revealed the unambiguous emergence of narrow He lines, confidently placing SN 2023emq in the more common Type Ibn class. Photometrically SN 2023emq has several uncommon properties regardless of its class, including its extreme initial decay (faster than $> 90\%$ of Ibn/Icn SNe) and sharp transition in the decline rate from $0.18\,\mathrm{mag/d}$ to $0.05\,\mathrm{mag/d}$ at $+20\,\mathrm{d}$. The bolometric light curve can be modelled as CSM interaction with $0.31 M_\odot$ of ejecta and $0.13 M_\odot$ of CSM, with $0.009 M_\odot$ of nickel, as expected of fast interacting SN. Furthermore, broad-band polarimetry at $+8.7$ days ($P = 0.55 \pm 0.30\%$) is consistent with high spherical symmetry. A discovery of a transitional Icn/Ibn SN would be unprecedented and would give valuable insights into the nature of mass loss suffered by the progenitor just before death, but we favour an interpretation that the emission lines in the classification spectrum are flash ionisation features commonly seen in young SNe the first days after the explosion. However, one of the features ($5700\,\text{Å}$) is significantly more prominent in SN 2023emq than in the few flash-ionised Type Ibn SNe and in that regard the SN is more similar to Icn SNe possibly implying continuum of properties between the two classes.

Keywords: (stars:) supernovae: general — (stars:) circumstellar matter

1. INTRODUCTION

The study of stellar explosions entered a new era in the wake of untargeted, high-cadence transient surveys allowing the discovery of transient phenomena that evolve on much faster timescales than typically expected of supernovae (SNe). Such rapidly evolving transients

(RETs) were first discovered in archival searches in surveys such as Pan-STARRS1 Medium Deep Survey (Drout et al. 2014) and Dark Energy Survey (Pursiainen et al. 2018; Wiseman et al. 2020), resulting in large samples of spectroscopically unclassified events. Even without classifications these events expanded our understanding of stellar deaths as their light curves evolved too fast to be explained by the decay of radioactive ^{56}Ni – the canonical power source of many typical SNe – and alternative power sources had to be considered.

In recent years an increasing number of fast events have been discovered in real time allowing intense follow-up campaigns. A significant number of them appear to be interacting H-poor SNe (e.g. Ho et al. 2023), either Type Ibn SNe characterised by a plethora of narrow helium emission lines (e.g. Foley et al. 2007; Pastorello et al. 2008), or Type Icn with emission lines of carbon and oxygen (e.g. Gal-Yam et al. 2022; Perley et al. 2022). While tens of Type Ibn SNe have been discovered over the last 15 years, so far only five Type Icn SNe have been identified all within the last four years. These are SN 2019hgp (Gal-Yam et al. 2022), SN 2019jc (Pellegrino et al. 2022a), SN 2021csp (Fraser et al. 2021; Perley et al. 2022), SN 2021ckj (Pellegrino et al. 2022a; Nagao et al. 2023) and SN 2022ann (Davis et al. 2023). Although not all Type Ibn are considered to be fast evolving (e.g. Inserra 2019), a significant subpopulation of SNe Ibn evolve on similar timescales to RETs, whilst all Icn SNe fall into this bright-and-fast parameter space.

The existence of transitional events that change type between Ibn and IIn supernovae over time (e.g. Pastorello et al. 2015a; Reguitti et al. 2022), suggests a continuum in the circumstellar material (CSM) properties of these events and consequently in the mass loss history of their progenitor stars. It may therefore be reasonable to expect that transitional events between non-hydrogen dominated CSM events (i.e. Type Icn to Ibn) also exist, although such events have not been identified to date. The discovery of such potential transitional events would be extremely valuable for our understanding of how massive stars lose their mass and create their CSM during their final stages giving insight into the chemical structure of the progenitor and the continuous or episodic nature of their mass loss.

Here we present an analysis of SN 2023emq, a SN initially identified as a Icn SN (Pellegrino et al. 2023), but which evolved to resemble a Ibn SN ~ 10 d later (Pursiainen & Leloudas 2023), making it potentially the first transitional Icn/Ibn SN to be identified. This paper is structured as follows: in Section 2 we present the observations and the data reduction procedures, in Section 3 we present the analysis of the data and in Section 4 we conclude our findings. The spectroscopy and photometry presented in this paper have been corrected for Milky Way extinction $E_{B-V} = 0.105$ (Schlafly & Finkbeiner 2011). Throughout the paper, we assume a flat ΛCDM cosmology with $\Omega_M = 0.3$ and $H_0 = 70$ km s^{-1} Mpc^{-1} and adopt redshift $z = 0.0338$.

2. OBSERVATIONS AND DATA REDUCTION

SN 2023emq was discovered by Asteroid Terrestrial-impact Last Alert System (ATLAS; Tonry et al. 2018; Smith et al. 2020) on 2023 Apr 01 under the name ATLAS23ftq, with a previous non-detection two days prior (Tonry et al. 2023). The SN is associated with LEDA797708 (Makarov et al. 2014), a visibly blue and irregular galaxy in Pan-STARRS1 3π images, with an offset of $\sim 6.2''$ from the brightest core region (Flewelling et al. 2020).

The photometry of SN 2023emq was collected from the public ATLAS and Zwicky Transient Facility (ZTF; Bellm et al. 2019) surveys, and with Target-of-opportunity observations with the Neil Gehrels Swift Observatory UV-Optical telescope (UVOT, PIs: Brown and Pellegrino). The late time ($\gtrsim +20$ d) evolution was monitored with aperture photometry from Alhambra Faint Object Spectrograph and Camera (ALFOSC) mounted on NOT at La Palma (PI: Pursiainen). The ATLAS o and c band light curves were generated using the ATLAS Forced Photometry service[1] (Shingles et al. 2021). The ZTF g and r band light curves were collected using the Alerce (Förster et al. 2021) and Lasair (Smith et al. 2019) brokers. The light curves from Swift UVOT were reduced following Charalampopoulos et al. (2023).

The spectra of SN 2023emq were obtained with NOT/ALFOSC, European Southern Observatory (ESO) Faint Object Spectrograph and Camera 2 (EFOSC2) on the New Technology Telescope (NTT) at La Silla observatory, Chile by the extended Public ESO Spectroscopic Survey for Transient Objects plus (ePESSTO+; Smartt et al. 2015) survey and X-Shooter (Vernet et al. 2011) at the Very Large Telescope (VLT) at the ESO Paranal observatory, Chile with a Director's Discretionary Time (DDT) Programme 2111.D-5006 (PI: Pursiainen). The NOT spectrum was reduced using the `PyNOT-redux` reduction pipeline,[2] the NTT spectrum with the PESSTO pipeline (Smartt et al. 2015) and the X-Shooter spectrum as described in Selsing et al. (2019). We also analysed the Global SN Project classification spectrum (Pellegrino et al. 2023) available in WISeREP[3] (Yaron & Gal-Yam 2012). Finally, we obtained one epoch of NOT/ALFOSC V-band imaging polarimetry on 2023 Apr 14 (+8.7 d). The data was reduced following Pursiainen et al. (2023).

3. ANALYSIS

3.1. *Photometry*

---

[1] fallingstar-data.com/forcedphot/

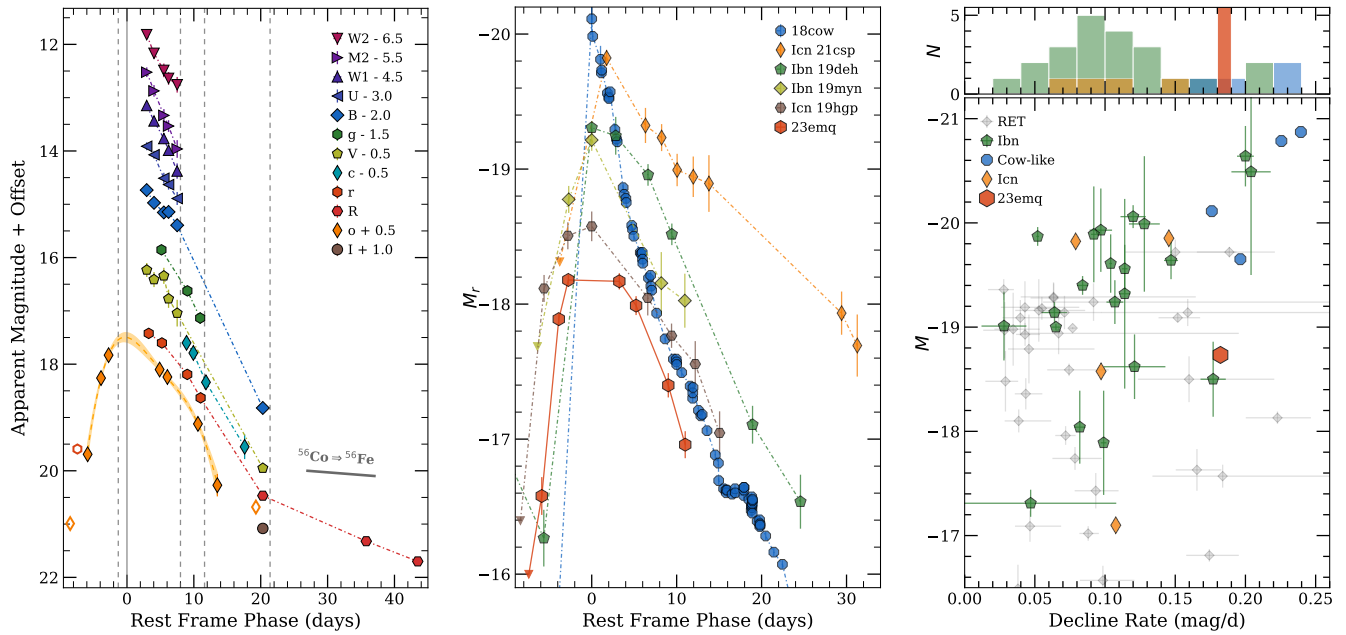[2] github.com/jkrogager/PyNOT/

[3] www.wiserep.org

Figure 1. Photometric qualities of SN 2023emq. Left: The multi-band light curve of SN 2023emq. Open markers refer non-detections (5σ). The spectral epochs are highlighted with dashed lines. The interpolated o-band GP light curve is shown over the data, and the decline rate of ^{56}Co is drawn for comparison. Middle: The ATLAS o-band light curve of SN 2023emq in comparison to r-band light curves of example fast events. The light curves are collected from ZTF via the Alerce broker (Förster et al. 2021) except for AT 2018cow where data presented in Prentice et al. (2018); Perley et al. (2019) was used. Right: Absolute magnitude vs. decline rate of fast-evolving transients. Values of Type Icn SNe (Pellegrino et al. 2022a), cow-like transients (Prentice et al. 2018; Perley et al. 2019; Ho et al. 2020; Perley et al. 2021; Yao et al. 2022) and SN 2023emq were obtained by fitting the first 20 d of post-peak r-band light curves linearly. The values for RETs are taken from Pursiainen et al. (2018), and the used bands (g, r, i or z) were chosen to be the closest to the rest frame r-band. Ibn SNe are collected from Hosseinzadeh et al. (2017), where data are presented mostly in R-band. On the top histogram we show the number (N) of transients per decline rate with SN 2023emq highlighted in red. No Icn SNe and only 2/22 Ibn are faster than SN 2023emq.

The multi-band light curve of SN 2023emq is shown in Figure 1 (left). While the decline is well covered, only the ATLAS o-band has pre-peak data. To estimate the peak MJD and magnitude we use Gaussian process (GP) interpolation using the setup presented in Pursiainen et al. (2020) and find the peak to be at MJD ~ 60040 and -18.7 ± 0.1 mag. To highlight the extreme evolution timescale of SN 2023emq, we compare its light curve to the enigmatic AT 2018cow and to example Icn/Ibn SNe chosen for their fast light curve evolution in Figure 1 (middle). While the rise of the SN is not exceptional, its initial decline is fast regardless of its type, and by the time of the last spectrum at $\sim +20$ d, the SN had already declined by 3.5 mag in brightness. In fact, the decline rate in the first 15 d post-peak (~ 0.18 mag/d) is at the extreme end of Ibn/Icn SNe and comparable to the events similar to AT 2018cow (e.g. Prentice et al. 2018; Perley et al. 2019; Ho et al. 2020; Perley et al. 2021; Yao et al. 2022), as demonstrated in Figure 1 (right). However, based on our NOT R-band data we can determine that after the observation at $+20$ d the decline slowed to 0.05 mag/d – nearly four times slower than the early decline. While the decline rates of Ibn SNe are ex-

pected to decrease in time and similar breaks have been seen before (e.g. SN 2015G; Shivvers et al. 2017), such extreme transitions are rare in the population (see e.g. Hosseinzadeh et al. 2017). Out of the Type Icn SNe, only SN 2022ann has exhibited a similar transition where the decline rate decreased from a maximum of ~ 0.14 mag/d to ~ 0.03 mag/d (Davis et al. 2023).

The late-time decline of SN 2023emq is faster than that expected from the ^{56}Co to ^{56}Fe decay (0.0098 mag/d), but the decay likely contributes at these epochs. Using the semi-analytical light curve models of Chatzopoulos et al. (2012, 2013), we fit the bolometric light curve of SN 2023emq (for details see Appendix A) with a combined CSM-interaction and nickel decay model. We assumed shell-like CSM with a setup presented by Pellegrino et al. (2022a) for type Icn SNe except for the opacity for which we used $\kappa = 0.2$ cm^{2}s^{-1} as appropriate for H-poor CSM (Chatzopoulos et al. 2013). As shown in Figure 2, we find a good fit with $M_{\rm CSM} = 0.13^{+0.01}_{-0.01} M_\odot$ and $M_{\rm ejecta} = 0.31^{+0.07}_{-0.03} M_\odot$ (1σ) with $M_{\rm Ni} = 0.009^{+0.002}_{-0.003} M_\odot$, but the decline needs to be followed longer to constrain the nickel mass. The recovered values of $M_{\rm CSM}$ and $M_{\rm ejecta}$ are smaller than
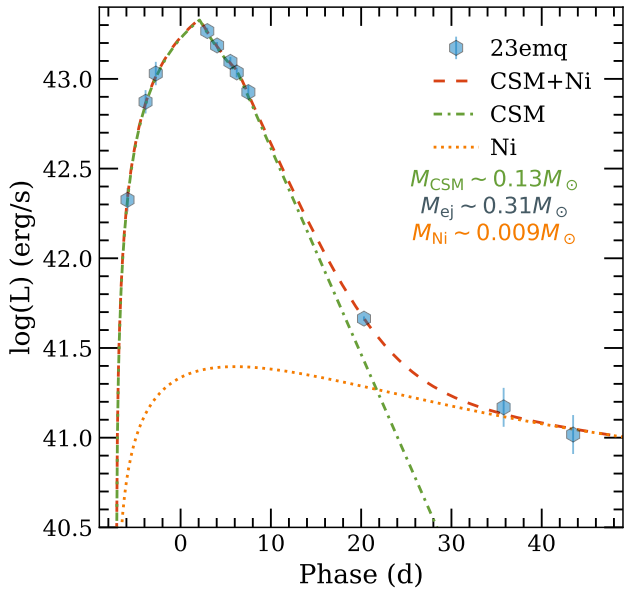
Figure 2. The best-fitting combined CSM and nickel decay model (Chatzopoulos et al. 2012, 2013) to the bolometric light curve of SN 2023emq. The derived CSM and ejecta masses are similar, but smaller in comparison to other Ibn/Icn SNe as expected given the fast light curve evolution near peak. The nickel mass is comparable to fast-evolving Ibn/Icn SNe, but the evolution needs to be monitored longer for it to be robustly constrained.

found in the literature for Type Ibn SNe (e.g. Pellegrino et al. 2022b), as expected given the fast photometric evolution. The M_{Ni} is similar to the lowest estimates for Type Ibn/Icn SNe (e.g. Pellegrino et al. 2022a).

3.2. *Spectroscopy*

The spectral time series of SN 2023emq is compared to example Type Ibn and Icn SNe, chosen based on their spectral similarity to SN 2023emq, in Figure 3. We adopt a redshift of $z = 0.0338$, determined based on host galaxy emission lines present in the 2D X-Shooter spectrum. In the classification spectrum, the most notable emission lines at 5700 Å and 4690 Å are identified as C III $\lambda5696$ and a blend of C III $\lambda4650$ and He II $\lambda4686$ (Pellegrino et al. 2023). These lines are common in Type Icn SNe, as demonstrated by well-studied SN 2019hgp (Gal-Yam et al. 2022), but emission at the similar wavelengths has also been seen in a few Type Ibn SNe (e.g. SN 2015U). In the subsequent spectra the SN has evolved into a typical Type Ibn SN characterised by strong He I emission lines. The spectra are virtually identical to that of Ibn SN 2014av shown in the figure.

The spectral evolution of the SN suggests that it could be a transitional Type Icn/Ibn SN, but the question relies on whether the early spectroscopic signatures are also seen in Type Ibn SNe, and important SNe to compare SN 2023emq to are the flash-ionised Type Ibn SNe

2010al (Pastorello et al. 2015a), 2019uo (Gangopadhyay et al. 2019) and 2019wep (Gangopadhyay et al. 2022). SNe often exhibit short-lived flash-ionised features early in their evolution as a result of CSM recombination after shock interaction between the ejecta and nearby CSM (e.g. Gal-Yam et al. 2014). All three SNe exhibit a strong emission feature at 4650 Å due to a blend of N III, C III and He II, as is typical for flash-ionised spectra of young SNe (see e.g. Khazov et al. 2016). However, while no emission is present at 5700 Å in SN 2010al, in SN 2019uo and SN 2019wep extremely faint C III $\lambda5969$ emission is reported. This is also the case for H-rich flash-ionised spectra, as the line is typically extremely faint if seen at all (e.g. SN 1998S; Fassia et al. 2001). In addition, Shivvers et al. (2016) showed that a similar but stronger emission line was also seen in an early spectrum of Type Ibn SN 2015U along the blended emission line at 4650 Å (see Figure 3). The authors identified the line as N II at $\lambda5680$, supported by the presence of several N II absorption lines in the later spectra (Pastorello et al. 2015b; Shivvers et al. 2016). Regardless of the exact identification of the line in SN 2023emq, emission has been detected at the two wavelengths in both Ibn and Icn SNe, and the presence of emission alone does not warrant a Icn classification.

In Figure 4 (left), we investigate what emission lines are present in the first spectrum in comparison to Ibn and Icn SNe. The line that best matches the feature at 4690 Å is He II, with a fainter contribution from N III/C III on the blue side of the feature. The presence of He II is indicative of Type Ibn SN, as in Type Icn the line is not prominent (e.g. Pellegrino et al. 2022a). Furthermore, the feature of Ibn SN 2015U appears to have the same shape as in SN 2023emq if the He II contribution is ignored while in Icn SNe C III $\lambda4650$ typically shows a P Cygni profile not seen in SN 2023emq. At 5700 Å the line is well-matched with both C III $\lambda5696$ and N II at 5680 Å and cannot be clearly distinguished. However, we remark that the emission in SN 2023emq is far more significant than in Ibn SNe 2015U and 2010al shown in the figure. While C III $\lambda5696$ emission was reported for two flash-ionised Ibn SNe (2019uo and 2019wep), the emission is visibly fainter than in SN 2015U (see Gangopadhyay et al. 2019, 2022). Instead, the emission line is prominent in Icn SNe. We searched the later spectra of SN 2023emq for signatures of C II or C I as seen in Icn SNe, but found no clear features. In the X-Shooter NIR spectrum, taken at +21.4 d, we identify a clear He I $\lambda10830$ emission line (4, right), but do not see the strong C I $\lambda10690$, detected in Icn SN 2021csp at a similar epoch (+20.5 d; Fraser et al. 2021).

To conclude, given the presence of the prominent He II emission in the first spectrum, the early spectral similarity to SN 2015U and the flash-ionised Type Ibn SNe as well as the unambiguous Ibn nature after peak brightness, we favour the interpretation that
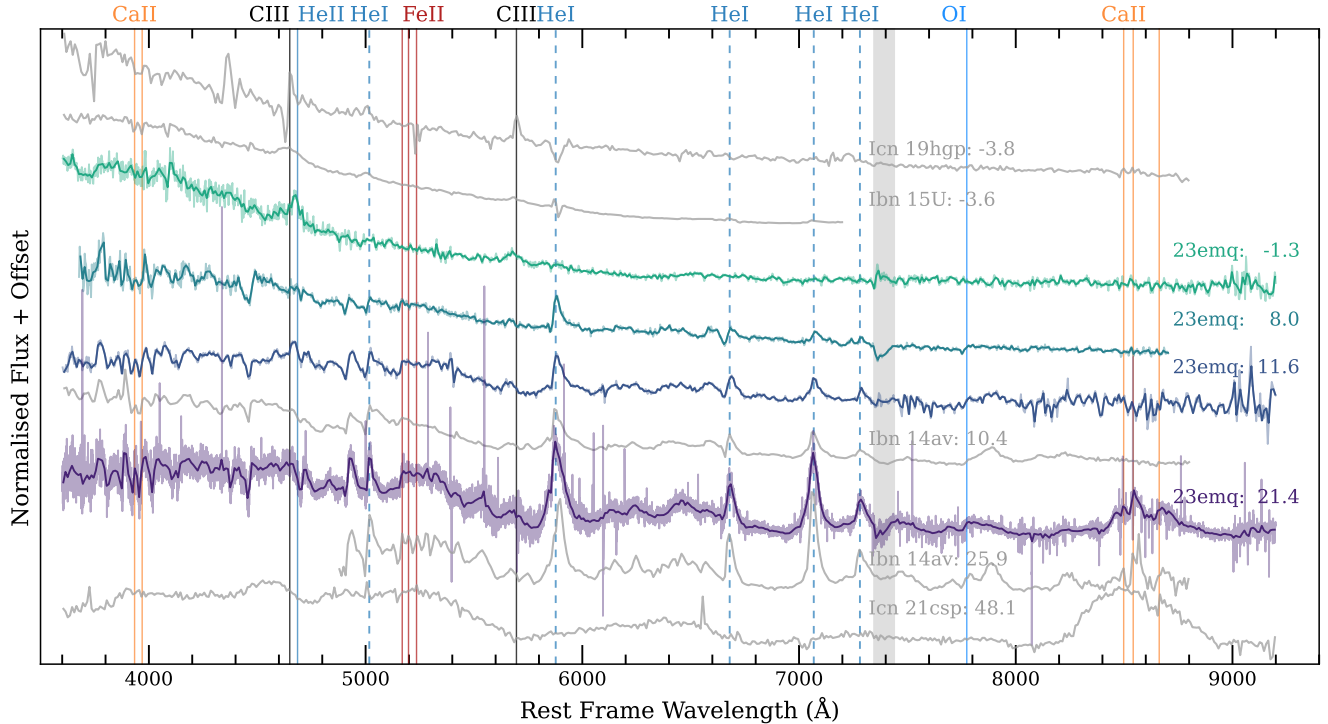
Figure 3. The spectroscopic time series of SN 2023emq (in colours) in comparison to the Type Icn SNe 2019hgp (Gal-Yam et al. 2022) and 2021csp (Perley et al. 2022), and the Type Ibn SNe 2015U (Shivvers et al. 2016) and 2014av (Pastorello et al. 2016) in grey. Spectral epochs are presented with respect to peak brightness. The first spectrum resembles that of SN 2015U and the latest spectrum is virtually identical to SN 2014av. As already noted by Perley et al. (2022), the continuum emission of SN 2021csp at late times is very similar to the continuum seen in Ibn SNe including SN 2023emq. The most prominent He I features are marked with dashed lines, and other strong features with solid lines. Note that the spectrum of the highly reddened SN 2015U is artificially flux-calibrated for visual comparison and that tellurics are shown in grey.

SN 2023emq is a flash-ionised Type Ibn SN. However, the unusually prominent emission line at 5700 Å might imply some kind of continuum between Icn and Ibn SNe and could indicate that the SN is either a transitional Type Ibn/Icn or a SN between the two populations.

We also used the X-Shooter spectrum to investigate the effect of host galaxy extinction. The Na I D doublet, which is typically used to estimate extinction in a galaxy, is not clearly visible in our high-resolution X-Shooter spectrum, and we can estimate the upper limit for $E_{\rm B-V}$ of the host by generating Gaussian absorption profiles over the spectrum. Assuming that the full width at half maximum of the line is the resolution of the spectrograph (35 km/s at 5890 Å), we find a 3σ limit for the total equivalent width of the doublet is EW ~ 0.146 Å. Using the empirical equation of Poznanski et al. (2012), this equates to $E_{\rm B-V} \lesssim 0.02$, indicating that the effect of the host galaxy extinction should be negligible.

3.3. Polarimetry

The polarimetry taken at +8.7 d shows that SN 2023emq is polarised as demonstrated in Figure 5 (right). We measure the dimensionless Stokes parameters to be $Q = -0.43 \pm 0.27\%$ and $U = 0.94 \pm 0.27\%$

corresponding to $P = 1.03 \pm 0.27\%$. In addition, it is possible to obtain measurements for two stars found in the ALFOSC field of view shown in Figure 5 (left). Both stars are bright, isolated targets, and based on the astrometric solutions from Gaia Data Release 3 (Gaia Collaboration et al. 2022) they also lie 150 pc above the Milky Way plane and should therefore be sufficiently far to probe the Milky Way dust content (Tran 1995). As such, they should be reliable estimators of the Galactic interstellar polarisation (ISP). The SN is clearly offset from the stars on the Q–U plane (Figure 5), which is an indication of intrinsic polarisation. Assuming the Galactic ISP can be obtained by averaging the two stars, we find Galactic ISP-corrected values for SN 2023emq of $Q = -0.24 \pm 0.30\%$ and $U = 0.37 \pm 0.30\%$, resulting in $P = 0.55 \pm 0.30\%$ (corrected for polarisation bias following Plaszczynski et al. 2014).

While we have no means to directly probe the host galaxy ISP, its maximum value should correlate with the host extinction following $P_{\rm ISP} < 9 \times E_{\rm B-V}$ (Serkowski et al. 1975). Using the derived limit on host extinction ($E_{\rm B-V} \lesssim 0.02$) we find that the effect of host galaxy dust content should be $P_{\rm ISP,Host} \lesssim 0.19\%$. As the derived polarisation degree ($P \sim 0.55\%$) is more signifi-
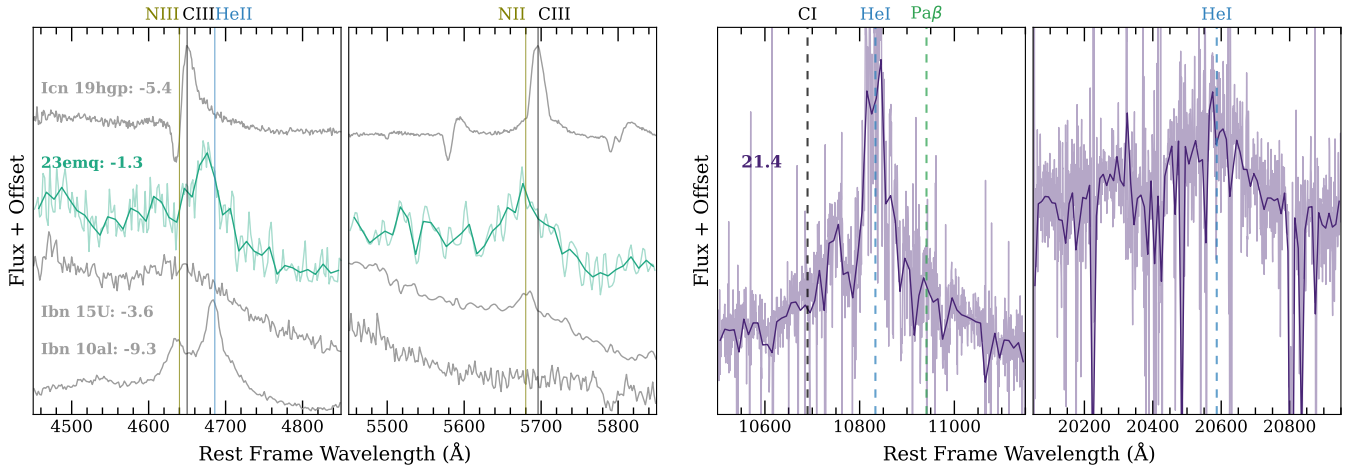
Figure 4. Left: The classification spectrum of SN 2023emq with the possible line identifications. The feature at 4690 Å is dominated by He II $\lambda 4686$ with faint blue excess possibly caused by either N III $\lambda 4640$ or C III $\lambda 4650$. At 5700 Å the emission could be either N II $\lambda 5680$ or C III $\lambda 5696$. Spectrum of SN 2015U from Figure 3 as well as early spectra of Icn SN 2019hgp (Gal-Yam et al. 2022) and flash-ionised Ibn SN 2010al (Pastorello et al. 2015a) are shown for comparison in grey. Around 4650 Å emission is seen in all of them. At 5700 Å the emission feature is either very faint (SN 2015U) or not seen (SN 2010al) in the Ibn SNe, but it is prominent in the Type Icn SN 2019hgp. Right: The only notable features in the X-Shooter NIR spectrum. He I $\lambda 10830$ is clear, but the strong C I emission line $\lambda 10690$ seen in Type Icn SN 2021csp (Fraser et al. 2021) is not present. He I $\lambda 20587$ is also tentatively identified.

cant, it is likely intrinsic to the SN. Given the spectrum at the time does not exhibit strong absorption lines that could induce polarisation (e.g. Wang & Wheeler 2008), the polarisation is likely that of the continuum. If the photosphere is an oblate ellipsoid, $P \sim 0.55\%$ corresponds to a lower limit of the physical minor over major axial ratio is $b/a \lesssim 0.9$ (Höflich 1991), but as shown by Pursiainen et al. (2022) the CSM can also be found in a disk/torus, and the CSM does not need to be in a uniform ellipsoidal shape. However, given the detection is not very strong, we conclude that the CSM shows high degree of spherical symmetry, in perhaps marginally aspherical configuration.

Polarimetry of Type Ibn/Icn SNe is very scarce in the literature, and polarimetric data that probes the intrinsic properties of the SNe has been presented only for one Ibn and one Icn SN. The spectral polarimetry obtained for Type Ibn SN 2015G 5 d after discovery showed $P \sim 2.7\%$, indicative of high asymmetry (Shivvers et al. 2017), while the one epoch for Type Icn SN 2021csp at $+3.5$ d shows low polarisation, implying high spherical symmetry (Perley et al. 2022). Additionally, Shivvers et al. (2016) presented three epochs of spectropolarimetry of the highly reddened Type Ibn SN 2015U at $\sim +5$ d and conclude that the observed polarisation signal was dominated by the contribution of dust in the host galaxy, and no firm conclusions on the polarisation of the SN were made. As such, our broad-band polarimetry for SN 2023emq is only the third observation that constrains the photospheric geometry of Ibn/Icn SNe. The H-poor CSM appears to often show high degree of spherical sym-

metry, but more events need to be observed to investigate the distribution of their photospheric shape.

4. CONCLUSIONS

We have presented an analysis of the photometric, spectroscopic and polarimetric properties of the fast evolving H-poor interacting SN 2023emq. While the rise of the SN is not particularly fast in the context of Type Ibn and Icn SNe, its initial decline (~ 0.18 mag/d) is remarkable and even comparable to AT 2018cow. After $+20$ d the decline rate slowed significantly to (~ 0.05 mag/d). Such a large transition in the decline rate is extreme and to our knowledge has not been seen before in interacting H-poor SNe. We modelled the bolometric light curve with a combined CSM interaction and nickel decay model and find good matches with $M_{\rm ejecta} \sim 0.31 M_\odot$ and $M_{\rm CSM} \sim 0.13 M_\odot$, with $\sim 0.009 M_\odot$ of ^{56}Ni. While the late-time light curve is still faster than expected of ^{56}Co to ^{56}Fe decay, it is likely that the radioactive decay is playing a part.

Spectroscopically the SN was initially classified as Type Icn based on the prominent emission features at 4650 Å and 5700 Å identified as C III as typical in Icn SNe (e.g. Gal-Yam et al. 2022; Perley et al. 2022). By $+8$ d, however, the SN had evolved into a typical Type Ibn characterised by prominent, narrow He I emission features. Such transition between Icn and Ibn would be unprecedented, but based on our analysis we conclude that SN 2023emq is likely a flash-ionised Ibn SN instead. As emission at 4650 Å and 5700 Å has been seen in a few Type Ibn SNe, just the presence of emission is not yet enough to classify the SN as Type Icn.
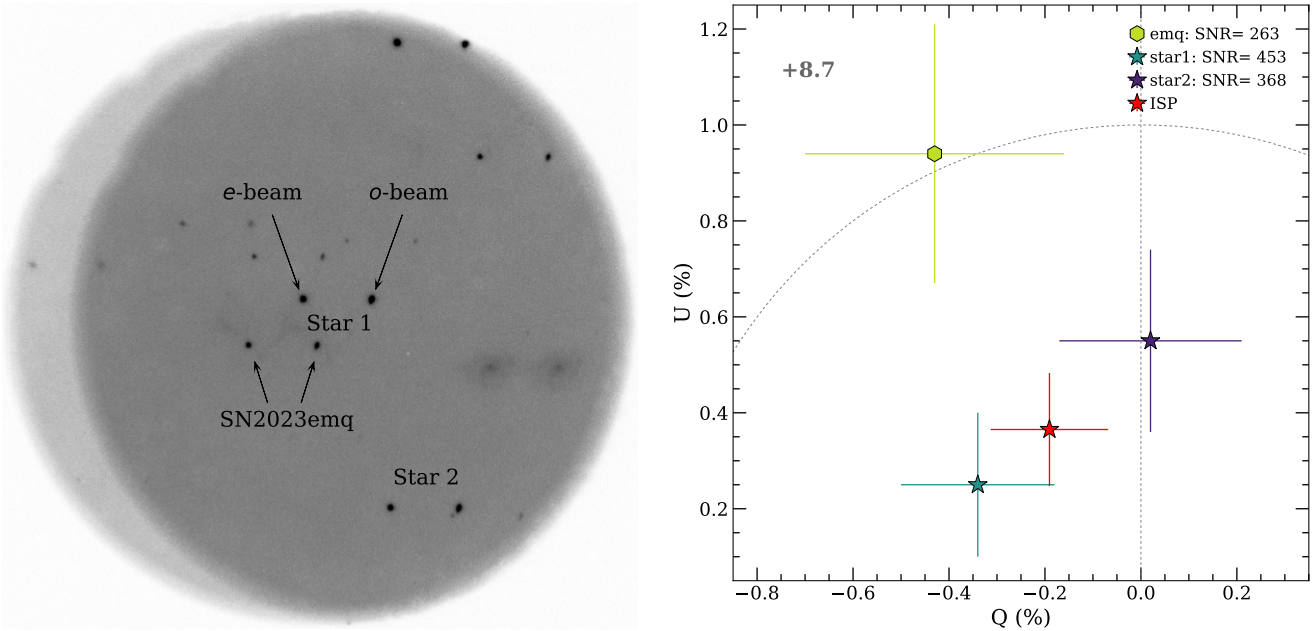
Figure 5. The NOT V-band polarimetry of SN 2023emq taken at $+8.7$ d post-peak. Left: The field of view of the observation. In the polarimetric mode, the extraordinary (e) and ordinary (o) beams are overlaid $15''$ apart. The SN and the two bright stars are marked. Other sources in the image were either too faint or too close to the edge for reliable estimation of the Stokes parameters. Right: The Stokes $Q-U$ plane. Both the SN and the two stars found in the image are shown. The SN is clearly offset from the stars. After correcting for the Galactic ISP and polarisation bias, we find intrinsic polarisation of $P = 0.55 \pm 0.30\%$. The dashed lines mark the location of $Q = 0\%$ and $P = 1\%$.

Line analysis revealed that the emission at 4650 Å seen in the first spectrum of SN 2023emq is dominated by He II with contribution from C III/N III, indicative of Ibn nature. Additionally, the C III $\lambda4650$ has typically a prominent P Cygni profile in Type Icn SNe, but only emission is present in SN 2023emq. While emission at 5700 Å has been seen in Type Ibn SNe (e.g. SN 2015U), it has always been far less prominent than that seen in SN 2023emq, and the emission feature resembles those seen in Type Icn SNe. In conclusion, we favour interpretation of flash-ionised nature for SN 2023emq, but the nature of the feature at 5700 Å could indicate that the SN is either a transitional Type Ibn/Icn or a SN between the two populations. More spectra obtained immediately after discovery are needed to investigate the importance of the emission at 5700 Å and further investigate the diversity of the flash-ionised features in core-collapse SNe.

We also obtained V-band polarimetry for SN 2023emq, making it only the third Type Ibn/Icn SNe with optical polarimetry that probed the intrinsic emission from the SN. We find polarisation degree $P = 0.55 \pm 0.30\%$ after correction for Galactic ISP and polarisation bias. Based on the upper limit on host extinction, the polarisation is likely not caused by the host dust content, and we conclude that the polarisation is intrinsic to the SN. Given the spectrum is dominated by interaction lines at the time, the result implies that

the CSM shows high spherical symmetry in possibly marginally aspherical configuration. More polarimetric observations of these SNe need to be obtained to characterise their geometric diversity and thus gain crucial insight to how the CSM is produced.

Facilities: NOT, VLT, Swift

Software: Astropy (Astropy Collaboration et al. 2013, 2018), Matplotlib (Hunter 2007), Numpy (Harris et al. 2020), SciPy (Virtanen et al. 2020), LMFIT (Newville et al. 2014), Astro-SCRAPPY (McCully et al. 2018), Source Extractor (Bertin & Arnouts 1996)

APPENDIX

A. BOLOMETRIC LIGHT CURVE

The bolometric light curve of SN 2023emq was constructed using blackbody fits to the multi-band epochs. The five epochs with UVOT data at $+3-8$ d and the NOT $BVRI$ epoch at $+20$ d were fit with a blackbody model to determine the evolution of temperature and radius shown in Figure 6. For these six epochs, we generated the bolometric luminosity assuming the spectral energy distribution is described by the blackbody fits. During the rise with only o-band data, we used the linearly declining temperature curve to estimate the temperature at the time of each data point and estimated the bolometric luminosity by scaling the resulting blackbody to the o-band magnitude. After $+20$ d, we adopted the temperature found at $+20$ d (~ 6500 K) and scaled the blackbody to the late-time R-band data. As such, our bolometric luminosity is well constrained only between $+3$ and $+20$ days. Outside this range the bolometric luminosities are uncertain and we have assumed 25% errors.

REFERENCES

Astropy Collaboration, Robitaille, T. P., Tollerud, E. J., et al. 2013, A&A, 558, A33, doi: 10.1051/0004-6361/201322068

Astropy Collaboration, Price-Whelan, A. M., Sipőcz, B. M., et al. 2018, AJ, 156, 123, doi: 10.3847/1538-3881/aabc4f

Bellm, E. C., Kulkarni, S. R., Barlow, T., et al. 2019, PASP, 131, 068003, doi: 10.1088/1538-3873/ab0c2a

Bertin, E., & Arnouts, S. 1996, A&AS, 117, 393, doi: 10.1051/aas:1996164

Charalampopoulos, P., Pursiainen, M., Leloudas, G., et al. 2023, A&A, 673, A95, doi: 10.1051/0004-6361/202245065

Chatzopoulos, E., Craig Wheeler, J., & Vinko, J. 2012, ApJ, 746, 121, doi: 10.1088/0004-637X/746/2/121

Chatzopoulos, E., Wheeler, J. C., Vinko, J., Horvath, Z. L., & Nagy, A. 2013, ApJ, 773, 76, doi: 10.1088/0004-637X/773/1/76

Davis, K. W., Taggart, K., Tinyanont, S., et al. 2023, MNRAS, 523, 2530, doi: 10.1093/mnras/stad1433

Drout, M. R., Chornock, R., Soderberg, A. M., et al. 2014, ApJ, 794, 23, doi: 10.1088/0004-637X/794/1/23

Fassia, A., Meikle, W. P., Chugai, N., et al. 2001, MNRAS, 325, 907, doi: 10.1046/j.1365-8711.2001.04282.x

Flewelling, H. A., Magnier, E. A., Chambers, K. C., et al. 2020, ApJS, 251, 7, doi: 10.3847/1538-4365/abb82d

Foley, R. J., Smith, N., Ganeshalingam, M., et al. 2007, ApJ, 657, L105, doi: 10.1086/513145
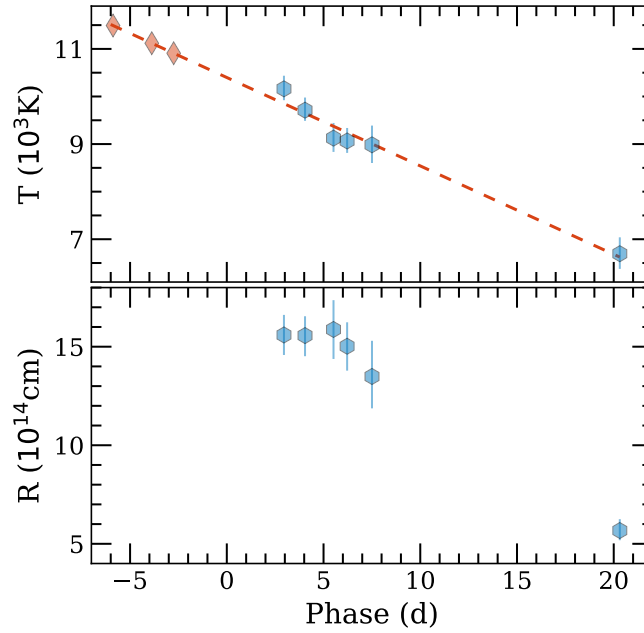
Figure 6. The temperature and radius evolution of SN 2023emq derived from blackbody fits to the six multi-band epochs (hexagons). The temperature is linearly declining, and the slope was used to determine the temperature at the time of *o*-band data points on the rise (diamonds).

Förster, F., Cabrera-Vives, G., Castillo-Navarrete, E., et al. 2021, AJ, 161, 242, doi: 10.3847/1538-3881/abe9bc

Fraser, M., Stritzinger, M. D., Brennan, S. J., et al. 2021, ArXiv e-prints, arXiv:2108.07278. https://arxiv.org/abs/2108.07278

Gaia Collaboration, Vallenari, A., Brown, A., & Prusti, T. 2022, A&A, 9, 10, doi: 10.1051/0004-6361/202243940

Gal-Yam, A., Arcavi, I., Ofek, E. O., et al. 2014, Nature, 509, 471, doi: 10.1038/nature13304

Gal-Yam, A., Bruch, R., Schulze, S., et al. 2022, Nature, 601, 201, doi: 10.1038/s41586-021-04155-1

Gangopadhyay, A., Misra, K., Hiramatsu, D., et al. 2019, ApJ, 889, 170, doi: 10.3847/1538-4357/ab6328

Gangopadhyay, A., Misra, K., Hosseinzadeh, G., et al. 2022, ApJ, 930, 127, doi: 10.3847/1538-4357/ac6187

Harris, C. R., Millman, K. J., van der Walt, S. J., et al. 2020, Array programming with NumPy, Nature Publishing Group, doi: 10.1038/s41586-020-2649-2

Ho, A. Y. Q., Perley, D. A., Kulkarni, S. R., et al. 2020, ApJ, 895, 49, doi: 10.3847/1538-4357/ab8bcf

Ho, A. Y. Q., Perley, D. A., Gal-Yam, A., et al. 2023, ApJ, 949, 120, doi: 10.3847/1538-4357/acc533

Höflich, P. 1991, A&A, 246, 481. https://ui.adsabs.harvard.edu/abs/1991A&A...246..481H/abstract

Hosseinzadeh, G., Arcavi, I., Valenti, S., et al. 2017, ApJ, 836, 158, doi: 10.3847/1538-4357/836/2/158

Hunter, J. D. 2007, Comput. Sci. Eng., 9, 90, doi: 10.1109/MCSE.2007.55

Inserra, C. 2019, Observational properties of extreme supernovae, doi: 10.1038/s41550-019-0854-4

Khazov, D., Yaron, O., Gal-Yam, A., et al. 2016, ApJ, 818, 3, doi: 10.3847/0004-637X/818/1/3

Makarov, D., Prugniel, P., Terekhova, N., Courtois, H., & Vauglin, I. 2014, A&A, 570, A13, doi: 10.1051/0004-6361/201423496

McCully, C., Crawford, S., Kovacs, G., et al. 2018, Zenodo, doi: 10.5281/ZENODO.1482019

Nagao, T., Kuncarayakti, H., Maeda, K., et al. 2023, A&A, 673, A27, doi: 10.1051/0004-6361/202346084

Newville, M., Ingargiola, A., Stensitzki, T., & Allen, D. B. 2014, Zenodo, doi: 10.5281/ZENODO.11813

Pastorello, A., Mattila, S., Zampieri, L., et al. 2008, MNRAS, 389, 113, doi: 10.1111/j.1365-2966.2008.13602.x

Pastorello, A., Benetti, S., Brown, P. J., et al. 2015a, MNRAS, 449, 1921, doi: 10.1093/mnras/stu2745

Pastorello, A., Tartaglia, L., Elias-Rosa, N., et al. 2015b, MNRAS, 454, 4293, doi: 10.1093/mnras/stv2256

Pastorello, A., Wang, X. F., Ciabattari, F., et al. 2016, MNRAS, 456, 853, doi: 10.1093/mnras/stv2634

Pellegrino, C., Howell, D. A., Terreran, G., et al. 2022a, ApJ, 938, 73, doi: 10.3847/1538-4357/AC8FF6

Pellegrino, C., Howell, D. A., Vinkó, J., et al. 2022b, ApJ, 926, 125, doi: 10.3847/1538-4357/ac3e63

10

Pellegrino, C., Gonzalez, E. P., Farah, J., et al. 2023, TNSAN, 75, 1. https://ui.adsabs.harvard.edu/abs/2023TNSAN..75....1P/abstract

Perley, D. A., Mazzali, P. A., Yan, L., et al. 2019, MNRAS, 484, 1031, doi: 10.1093/mnras/sty3420

Perley, D. A., Ho, A. Y. Q., Yao, Y., et al. 2021, MNRAS, 508, 5138, doi: 10.1093/mnras/stab2785

Perley, D. A., Sollerman, J., Schulze, S., et al. 2022, ApJ, 927, 180, doi: 10.3847/1538-4357/ac478e

Plaszczynski, S., Montier, L., Levrier, F., & Tristram, M. 2014, MNRAS, 439, 4048, doi: 10.1093/MNRAS/STU270

Poznanski, D., Prochaska, J. X., & Bloom, J. S. 2012, MNRAS, 426, 1465, doi: 10.1111/j.1365-2966.2012.21796.x

Prentice, S. J., Maguire, K., Smartt, S. J., et al. 2018, ApJ, 865, L3, doi: 10.3847/2041-8213/aadd90

Pursiainen, M., & Leloudas, G. 2023, TNSAN, 88. https://ui.adsabs.harvard.edu/abs/2023TNSAN..88....1P/abstract

Pursiainen, M., Childress, M., Smith, M., et al. 2018, MNRAS, 481, 894, doi: 10.1093/MNRAS/STY2309

Pursiainen, M., Gutiérrez, C. P., Wiseman, P., et al. 2020, MNRAS, 494, 5576, doi: 10.1093/mnras/staa995

Pursiainen, M., Leloudas, G., Paraskeva, E., et al. 2022, A&A, 666, A30, doi: 10.1051/0004-6361/202243256

Pursiainen, M., Leloudas, G., Cikota, A., et al. 2023, A&A, 674, A81, doi: 10.1051/0004-6361/202345945

Reguitti, A., Pastorello, A., Pignata, G., et al. 2022, A&A, 662, L10, doi: 10.1051/0004-6361/202243340

Schlafly, E. F., & Finkbeiner, D. P. 2011, ApJ, 737, 103, doi: 10.1088/0004-637X/737/2/103

Selsing, J., Malesani, D., Goldoni, P., et al. 2019, A&A, 623, A92, doi: 10.1051/0004-6361/201832835

Serkowski, K., Mathewson, D. L., & Ford, V. L. 1975, ApJ, 196, 261, doi: 10.1086/153410

Shingles, L., Smith, K. W., Young, D. R., et al. 2021, TNSAN, 7, 1. https://ui.adsabs.harvard.edu/abs/2021TNSAN...7....1S/abstract

Shivvers, I., Zheng, W., Mauerhan, J., et al. 2016, MNRAS, 461, 3057, doi: 10.1093/mnras/stw1528

Shivvers, I., Zheng, W. K., Van Dyk, S. D., et al. 2017, MNRAS, 471, 4381, doi: 10.1093/MNRAS/STX1885

Smartt, S. J., Valenti, S., Fraser, M., et al. 2015, A&A, 579, 6, doi: 10.1051/0004-6361/201425237

Smith, K. W., Williams, R. D., Young, D. R., et al. 2019, Res. Notes AAS, 3, 26, doi: 10.3847/2515-5172/ab020f

Smith, K. W., Smartt, S. J., Young, D. R., et al. 2020, PASP, 132, 1, doi: 10.1088/1538-3873/ab936e

Tonry, J., Denneau, L., Weiland, H., et al. 2023, TNSTR, 2023-698, 1. https://ui.adsabs.harvard.edu/abs/2023TNSTR.698....1T/abstract

Tonry, J. L., Denneau, L., Heinze, A. N., et al. 2018, PASP, 130, doi: 10.1088/1538-3873/aabadf

Tran, H. D. 1995, ApJ, 440, 565, doi: 10.1086/175296

Vernet, J., Dekker, H., D'Odorico, S., et al. 2011, A&A, 536, A105, doi: 10.1051/0004-6361/201117752

Virtanen, P., Gommers, R., Oliphant, T. E., et al. 2020, Nat. Methods, 17, 261, doi: 10.1038/s41592-019-0686-2

Wang, L., & Wheeler, J. C. 2008, ARA&A, 46, 433, doi: 10.1146/annurev.astro.46.060407.145139

Wiseman, P., Pursiainen, M., Childress, M., et al. 2020, MNRAS, 498, 2575, doi: 10.1093/mnras/staa2474

Yao, Y., Ho, A. Y. Q., Medvedev, P., et al. 2022, ApJ, 934, 104, doi: 10.3847/1538-4357/AC7A41

Yaron, O., & Gal-Yam, A. 2012, PASP, 124, 668, doi: 10.1086/666656